Role of the Large Cytoplasmic Loop of the α7 Neuronal Nicotinic Acetylcholine Receptor Subunit in Receptor Expression and Function†

Luis M. Valor, José Mulet, Francisco Sala, Salvador Sala, Juan J. Ballesta, and Manuel Criado*

Instituto de Neurociencias, Universidad Miguel Hernández-CSIC, Campus de San Juan, 03550-San Juan (Alicante) Spain

Received March 18, 2002; Revised Manuscript Received May 2, 2002

ABSTRACT: The role of the large intracellular loop of the nicotinic acetylcholine receptor (nAChR) α7 subunit in the expression of functional channels was studied. For this purpose, systematic deletions and substitutions were made throughout the loop and the ability of the mutated α7 subunits to support expression of functional nAChRs at the *Xenopus* oocyte membrane was tested. Surface nAChR expression was abolished upon removal of sequences at two regions, a 29-amino acid segment close to the N-terminus of the loop (amino acids 297−325) and adjacent to the third transmembrane region and an 11-amino acid segment near the fourth transmembrane region. Some residues (amino acids 317−322) within the 29 amino acids N-terminal segment could be substituted by others but not deleted without loss of expression, suggesting that a certain structure, determined by the number of amino acids rather than by their identity, has to be maintained in this region. The contiguous sequence M323 K324 R325 did not tolerate deletions and substitutions. Removal of the rest of the cytoplasmic loop was not deleterious; even higher expression levels (2−4-fold) were obtained upon large deletions of the loop (Δ399−432 and Δ339−370). High expression levels were observed provided that a minimal sequence of three amino acids (E371, G372, and M373) was present. In addition, some electrophysiological properties of mutant nAChRs were modified. Substitution of the EGM sequence by other protein segments produced a variety of effects, but, in general, insertions were not well tolerated, suggesting the existence of tight structural restrictions in the large cytoplasmic region of the rat α7 subunit.

Neuronal nicotinic acetylcholine receptors (nAChR)[1] are members of a supergene family of ion channels gated by neurotransmitters (*1*). They are pentameric oligomers composed of related glycoprotein subunits, each one composed of ∼500 amino acids and four transmembrane segments (*2*, *3*). About 210 amino acids at the N-terminus form the major extracellular domain. This domain is well conserved among subunits and contains elements specific for ligand binding and subunit assembly and recognition (*4*). The other large domain is located intracellularly between the third and fourth transmembrane regions and has considerable sequence and length variability. It has been shown to be involved in nAChR assembly (*5*), targeting (*6*, *7*), and trafficking (*8*), and may also encode signals for nAChR phosphorylation (*9*, *10*).

nAChRs formed by α7 subunits are widely expressed in the central and peripheral nervous systems (*11*). Their high Ca^{2+} permeability suggests their involvement in neuronal growth, differentiation, plasticity, and other Ca^{2+}-dependent mechanisms (*12*). In heterologous expression systems, α7 subunits form homomeric nAChRs and seem unable to assemble with other subunits (*13*). Immunoprecipitation studies also indicate that α7 subunits do not seem to be associated with previously cloned subunits (*14*). This different association behavior may reflect the existence of specific features in the structure of this subunit (*15*). In fact, we have previously shown that homomer formation requires compatibility between amino acid residues of the M1 and M2 transmembrane segments (*16*). We have now extended these studies to the highly variable cytoplasmic loop to show that only relatively short loop stretches, immediately adjacent to M3 and M4 transmembrane segments are required for α7 nAChR expression. These minimal requirements contrast, however, with the inability of α7 loop to accommodate other protein segments, related or not to the nAChR supergene family, suggesting the existence of structural restrictions in this region of the α7 subunit.

EXPERIMENTAL PROCEDURES

Generation of Constructs of the Rat α7 Subunit. The rat α7 cDNA was cloned in the pBluescript vector and in a derivative of the pSP64T vector (*17*) containing part of the pBluescript polylinker. The appropriate DNA cassettes were generated by PCR and used to substitute original segments of the α7 subunit, by using restriction enzyme digestions. For this purpose, we used restriction enzyme sites present in the original cDNA sequence such as an *Eco*RV site, corresponding to amino acids R294 and Y295 just at the N-terminal end of the cytoplasmic loop, and an *Sph*I site at

† This work was supported by grants from the ministry of Education (DGCYT, PM98-0104 and PM98-0097). L.M.V. was the recipient of a predoctoral fellowship from Generalitat Valenciana.

* To whom correspondence should be addressed at Instituto de Neurociencias, Universidad Miguel Hernández-CSIC, Campus de San Juan, 03550-San Juan (Alicante), Spain. Telephone: +34 965919479. Fax: +34 965919484. E-mail: manuel.criado@umh.es.

[1] Abbreviations: ACh, acetylcholine; α-Bgt, α-bungarotoxin; GFP, green fluorescent protein; mAb, monoclonal antibody, nAChR, nicotinic acetylcholine receptor.

10.1021/bi025831r CCC: $22.00
Published on Web 06/04/2002

the middle of the loop, at positions G372 and M373. In addition, silent mutations were introduced to generate two restriction enzyme sites: an ACG CGT *Mlu*I site corresponding to amino acids T309 and R310, also close to the N-terminal end of the loop, and a C ATA TG *Nde*I site involving amino acids V433, I434, and C435, at the C-terminal region of the loop. To generate the shortest constructs (constructs 15−28), we annealed single-stranded oligonucleotides with the desired sequences and proper single strand ends which could be easily ligated to the ends generated by the restriction enzymes mentioned above. Finally, to assemble the chimeric subunits made with different proteins, an intermediate construct (construct 29) was generated by cloning a linker with the following sequence: 5′-CCC ATG GGT CTA GAA GAT CTA-3′ coding for amino acids: PMGLEDL. This linker contained *Nco*I and *Bgl*II sites which were used to clone the complete green fluorescent protein (GFP) DNA obtained from the pEGFP-C3 plasmid (Clontech) with the same enzymes and also the cDNA coding for the whole SNAP-25 protein (generously provided by Dr. C. Bark). The DNAs coding for the cytoplasmic loops of the rat α4 and α5 subunits were generated by PCR of the original cDNAs (generously provided by Dr. J. Patrick) and introduced into the α7 construct lacking amino acids 326−432 in order to replace them.

Oocyte Expression. Capped mRNA was synthesized in vitro using SP6 RNA polymerase, the mMESSAGEmMACHINE kit (Ambion, Texas) and the pSP64T derivative mentioned above. Defoliculated *Xenopus leavis* oocytes were injected with 5 ng of total cRNA in 50 nL of sterile water. All experiments were performed within 3−4 days after cRNA injection. Wild-type α7 mRNA was injected into oocytes from the same frog every time a mutant was tested. Consequently, mutant expression was expressed as a percentage of wild-type α7 expression observed in the same experiment.

[^{125}I]-α-Bungarotoxin (α-Bgt) Binding Assays. Specific surface expression of [^{125}I]-α-Bgt binding sites was tested with 5 nM [^{125}I]-α-Bgt as described (*18*). Briefly, oocytes were incubated with 5 nM [^{125}I]-α-Bgt for 1 h at room temperature. At the end of the incubation, unbound [^{125}I]-α-Bgt was removed, oocytes were washed, and bound radioactivity was counted. Nonspecific binding was determined using noninoculated oocytes. To measure total [^{125}I]-α-Bgt binding sites, oocytes were solubilized as described in Anand et al. (*19*), and the oocyte extract was incubated with 5 nM [^{125}I]-α-Bgt for 2 h. Then, the extract was immunoprecipitated with mAb 319, a monoclonal antibody specific for the α7 subunit (*20*).

Electrophysiological Recordings. Electrophysiological recordings were done as previously described (*18*). Functional expression of each construct was estimated as the peak ionic current evoked by 1 s application of 1 mM ACh at −80 mV.

Confocal Microscopy. Oocytes were injected with RNA corresponding to construct 30, which contains the whole GFP inserted into the cytoplasmic region of the α7 subunit. Three days later, injected oocytes were placed in a Petri dish bathed with normal frog Ringer, and pictures were taken with a Zeiss LSM510 confocal microscope with a 10× objective, usually with an optical section of approximately 50 μm, although this value may change from one picture to another. Control oocytes injected with α7 RNA were treated in the same way. Autofluorescence of the oocyte yolk was very low in control oocytes (see Figure 7 for a comparison between oocytes injected with construct 30 and α7 subunit RNAs in the same conditions); therefore, nothing special was used to prevent it.

RESULTS

Effects of Large Deletions of the Cytoplasmic Loop on α7 nAChR Expression. Expression of functional nAChRs was monitored in two ways: by measuring α-Bgt binding to the external surface of oocytes and by recording the ionic currents evoked using acetylcholine. Constructs with loop deletions might differ in their apparent affinity for ACh (see below); therefore, α-Bgt binding experiments complemented the use of the current evoked by 1 mM ACh to test functional expression. Moreover, it is important to note that we used α7 nAChR expression as a parallel control in all experiments because of the inherent variability of the oocyte expression system: the results are expressed as a percentage of the α7 response.

As an initial approach to determine the contribution of the cytoplasmic loop of the α7 subunit on the formation of functional nAChRs, we studied the expression of constructs in which large areas of the loop had been deleted (Figure 1). Segments of the cytoplasmic loop immediately adjacent to transmembrane fragments M3 and M4 contain amino acid sequences that are highly conserved among nAChR subunits. When these segments (amino acids 297−310 and 437−447 in constructs 1 and 2, respectively) were deleted, no nAChR expression was observed (Figure 1B). Therefore, these regions appear to be essential for nAChR expression and were left intact in further constructs. The rest of the cytoplasmic loop was divided in four parts of approximately the same length (boxes labeled 1 to 4 in the lowest part of Figure 1B). The simultaneous deletion of these regions abolished nAChR expression (construct 3, Figure 1B). The same happened when regions 1 and 2 or even region 1 alone were eliminated (constructs 4 and 5, respectively, Figure 1B). These results suggest that region 1 (amino acids 311−338) contains elements needed for nAChR expression. The role of the other segments was further studied with additional constructs. Surprisingly, when region 4 (amino acids 399−432) was eliminated, expression of nAChRs was about 2-fold higher than that observed for wild-type α7 subunits. Moreover, a construct with regions 2 and 4 simultaneuously deleted (construct 7, Figure 1B) expressed about 4-fold more functional nAChRs than the α7 subunit. In contrast, the simultaneous deletion of regions 1 and 4 abolished nAChR expression (construct 8, Figure 1B), thus confirming the essential role of region 1. Since the construct yielding the highest level of expression contained regions 1 and 3 (construct 7), we decided to delete region 3, therefore leaving a cytoplasmic loop composed of only region 1 (contruct 9, Figure 1B). In this case, expression levels were similar to those observed for the wild-type α7 subunit nAChR, suggesting that the deleted segments are not needed for nAChR expression, although higher expression levels are retained in its presence. The increase observed with construct 7 could result from a higher incorporation of nAChRs at the oocyte surface membrane, while the total amount of nAChR

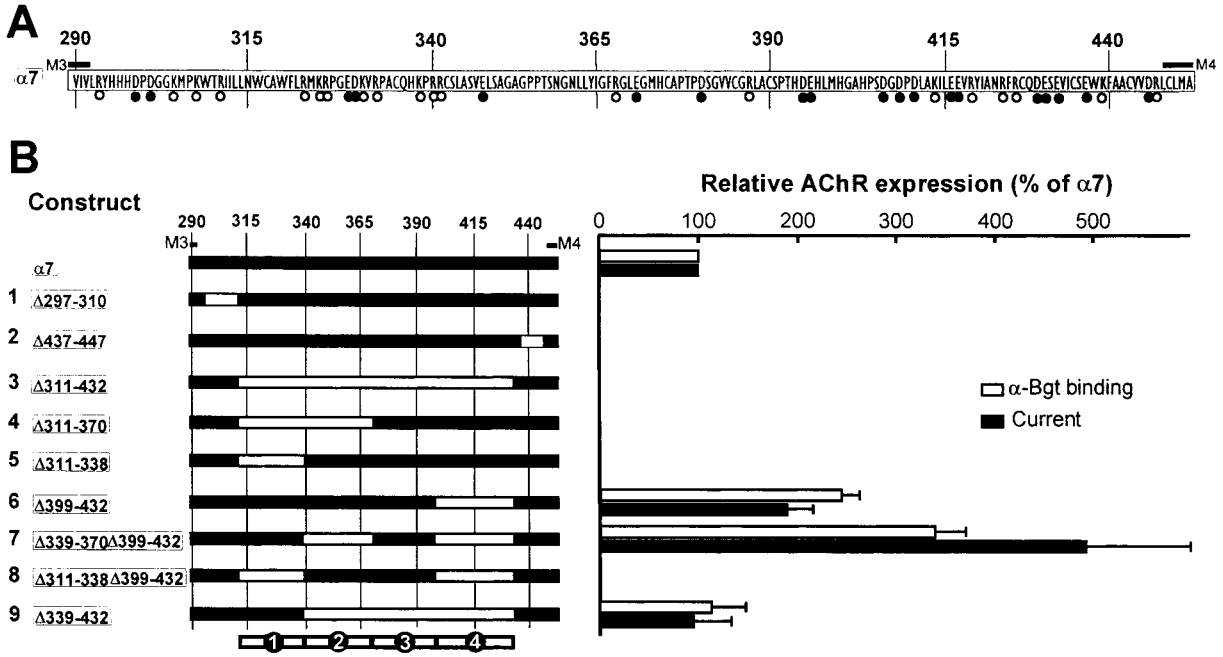

FIGURE 1: Effect of large deletions of the cytoplasmic loop on the expression of functional α7 nAChRs. (A) The sequence of the long cytoplasmic loop of the α7 subunit is shown with the numbering used throughout this study. Positively and negatively charged amino acids are indicated by open and closed circles, respectively. (B) Schematic diagram of the structures of deleted α7 subunits and their functional expression at the oocyte membrane. The cytoplasmic loop of each mutated subunit is displayed with the deleted regions indicated by open boxes. The diagram at the botton shows the four domains (1−4) that were initially considered in this study. Expression of the different constructs was tested by α-Bgt binding (open boxes) and by the extent of the ionic currents evoked by application of 1 mM ACh (closed boxes). All data were normalized to those obtained with the wild-type α7 subunit, and means ± SEM of at least three experiments from different donors (20 oocytes/experiment) are shown. Typical values obtained with the α7 subunit were ~1 fmol of bound α-Bgt/oocyte and ~2 μA/oocyte at −80 mV.

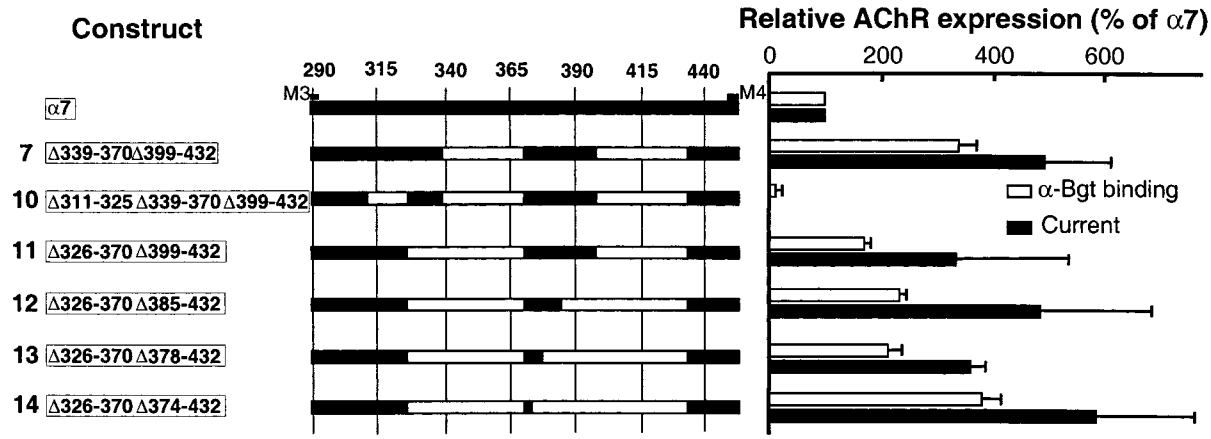

FIGURE 2: Mapping of loop regions composed by amino acids 311−338 and 371−398 of the α7 subunit. A schematic diagram of the constructs used to map in more detail domains 1 and 2 is shown at the left. The data were expressed as indicated in the legend of Figure 1. The expression data of construct 7 were included for comparative purposes.

synthesized remained unaltered. To test this possibility, we measured total [^{125}I]-αBgt binding sites by immunoprecipitating them with an α7 specific mAb (mAb 319). The mAb 319 epitope was previously mapped to amino acids 365−384 (*21*) in the chicken α*7* subunit and probably recognizes the analogous sequence in the rat subunit because its cross-reaction (*11*). Construct 7 lacks the first six amino acids of the epitope; however, the remaining protein stretch (amino acids 371−384) seems to contain sufficient binding elements to promote antibody recognition. Thus, mAb 319 immunoprecipitated ~4−5-fold more total nAChRs from construct 7 than from α7, the percentage of surface nAChRs being similar, ~70% of the total amount (results not shown). Therefore, changes in surface expression levels are not due to nAChR reallocation between intracellular and surface pools, i.e., modifications of a nAChR transport mechanism.

Further Mapping of Regions 1 (Amino Acids 311−338) and 3 (Amino Acids 371−398). With the aim of mapping more accurately which elements within regions 1 and 3 contribute to α7 nAChR expression, we assembled additional constructs in the context of construct 7, the one producing the maximal expression level. No expression was observed upon deletion of the N-terminal half of region 1 (construct 10, Figure 2), whereas deletion of the C-terminal half did not affect nAChR expression, since construct 11 (Figure 2) gave rise to about 2-fold more functional nAChRs than the native α7 subunit. Therefore, in region 1 the sequence between amino acids 311−325 appeared important for

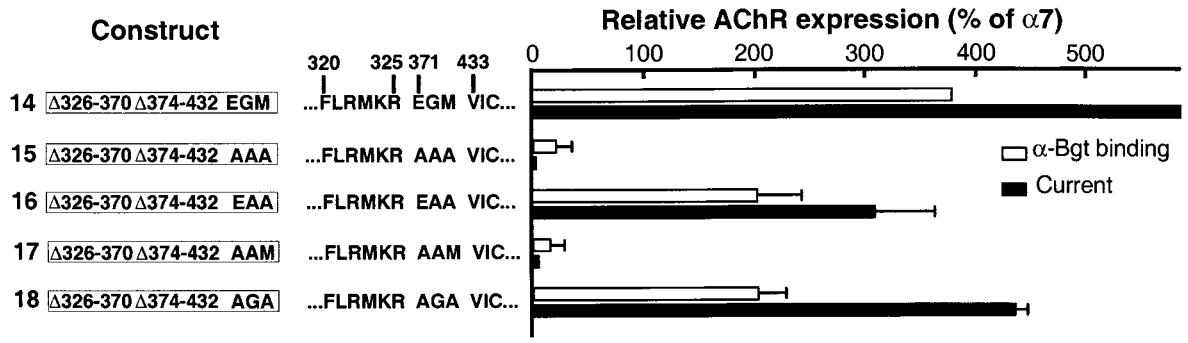

FIGURE 3: Mutational study of the sequence E371G372 M373 of the α7 subunit. Amino acids E371, G372, and M373 were mutated to alanines in the context of construct 14, as indicated at the left part of the figure. Data obtained with construct 14 are also included for comparative purposes. The data were expressed as indicated in the legend of Figure 1.

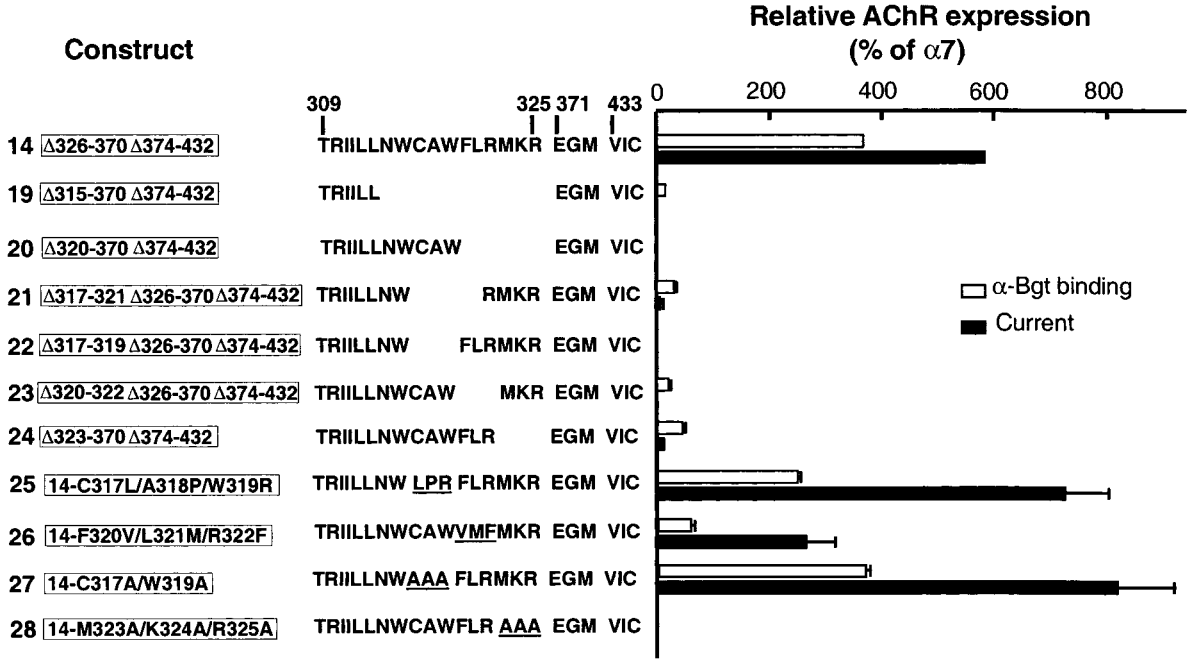

FIGURE 4: Mapping of region comprising amino acids 311−325 of the α7 subunit. A schematic diagram of the constructs used to map in more detail this region is shown at the left. Several amino acids were deleted (constructs 19−24) or mutated (constructs 25−28), and the effect on expression of functional nAChRs was studied. The data were expressed as indicated in the legend of Figure 1.

nAChR expression and was dissected further (see Figure 4). Regarding region 3, we performed succesive C-terminal deletions (constructs 12−14) until leaving only the three most N-terminal residues (construct 14). All constructs produced functional nAChRs at a level similar to construct 7, and, therefore, the presence of only three amino acids E371, G372, and M373 in construct 14 seemed sufficient to maintain expression at higher levels. This effect could be specific to the mentioned amino acids or perhaps the consequence of keeping this part of the cytoplasmic loop with a critical length. For this reason, we substituted them by alanines (Figure 3). Thus, when the three amino acids were mutated simultaneously, only a small amount of nonfunctional nAChRs was present at the oocyte surface membrane (about 30% of α-Bgt binding sites found with α7 but no current, construct 15, Figure 3). The same happened with the double mutant E371A/G372A (construct 17). By contrast, the double mutants G372A/M373A (construct 16) and E371A/M373A (construct 18) produced about 2-fold more functional nAChRs than the wild-type α7 subunit. These results suggest that the presence of either E371 or G372 but not M373 is required for nAChR expression. However, these requirements are probably the minimal ones but do not appear to be unique, as other sequences could play a similar role as shown below (see construct 29, Figure 6).

Regarding the sequence between amino acids 311−325, which was considered essential to express functional nAChRs (construct 10, Figure 2), it was further mapped by deleting segments within it. Thus, deletion of amino acids 315−325 was deleterious for nAChR expression (construct 19, Figure 4), and the same was true for smaller deletions such as Δ320−325 (construct 20), Δ317−321 (construct 21), Δ317−319 (construct 22), Δ320−322 (construct 23), and Δ323−325 (construct 24). Therefore, it seems that the whole region between amino acids 315 and 325 is needed for nAChR expression. Interestingly, if amino acids 317−319 or 320−323 were substituted by their analogous counterparts in the α3 subunit (constructs 25 and 26, respectively), functional expression, although lower than that obtained with the original α7 sequence, was observed, suggesting that a determined structure supported by a defined number of amino acids is needed in this region, independently of their identity. In fact, substitution of amino acids 317 and 319 just by alanines (construct 27) produced the highest expression of

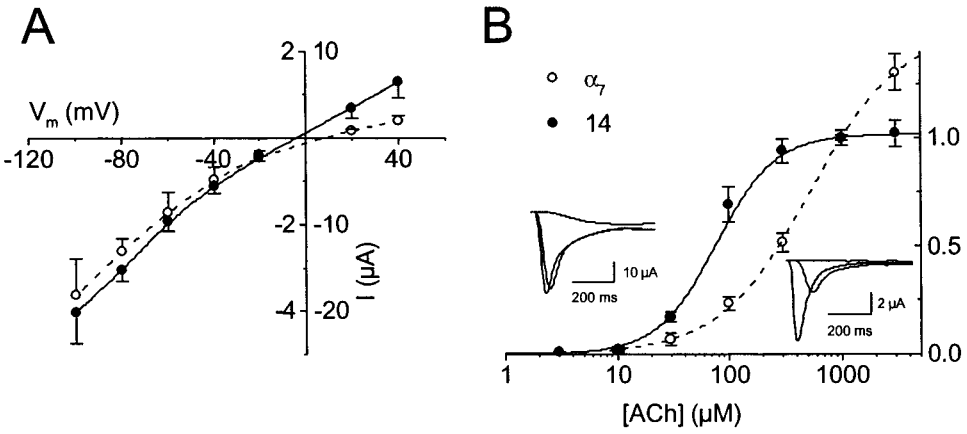

FIGURE 5: Current−voltage and dose−response curves for α7 and construct 14. (A) Peak current−voltage relationship for α7 (open circles, dashed line) and construct 14 (closed circles, continuous line). Note that the current scale for construct 14 (from 10 to −25 μA) is 5 times larger than for α_7 (from 2 to −5 μA). Data points are joined simply by spline lines. Pulses of 1 mM ACh were used for both nAChRs. (B) Dose−response curves for α7 (open circles, dashed line) and construct 14 (solid circles, continuous line). For each nAChR, peak currents were normalized to the value obtained with 1 mM ACh. Lines are fits to the Hill equation with the following parameters (I/I_{max}, EC_{50}, n Hill) for α7: (1.49 ± 0.07, 520 ± 55 μM, 1.08 ± 0.04), for construct 14: (1.01 ± 0.02, 77 ± 12 μM, 1.65 ± 0.16). Membrane potential was −80 mV. Insets show current records for α7 (right) and construct 14 (left) obtained with 30, 300, and 3000 μM ACh. In both panels, data points are averages of 7−30 oocytes from at least two donors. Error bars are standard errors.

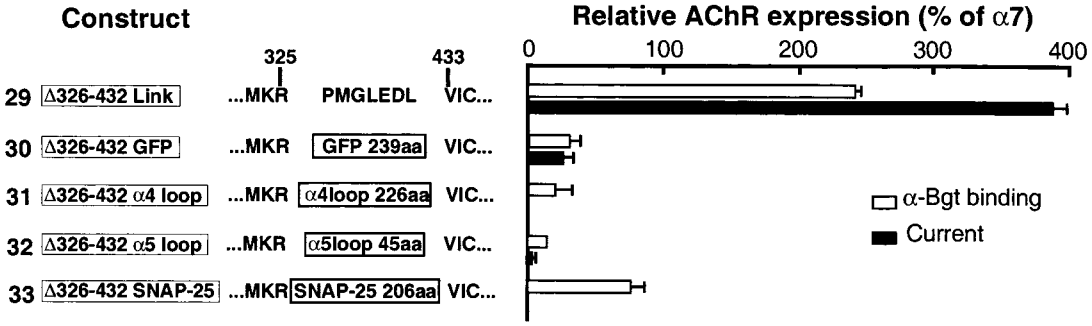

FIGURE 6: Effects of substituting the α7 loop by other proteins. The region between amino acids 326 and 432 of the α7 subunit was substituted by segments of other proteins such as the whole GFP (construct 30) and SNAP-25 (construct 33) proteins or the corresponding cytoplasmic regions of the nAChR α4 (construct 31) and α5 (construct 32) subunits. A construct with seven amino acids, used as an intermediate to insert the GFP and SNAP-25 proteins, was also tested (construct 29). The inserted α4 loop sequence corresponds to amino acids 364−589 of the rat α4 subunit, whose N- and C-terminal ends are PSV... and ...TDF, respectively. The sequence MKR (amino acids 323−325 of the α7 subunit) is also present at the α4 subunit. The inserted α5 loop sequence corresponds to amino acids 354−398 of the rat α5 subunit, whose N- and C-terminal ends are HAD... and ...DVR, respectively. The data were expressed as indicated in the legend of Figure 1.

all constructs. By contrast, the role of amino acids 323−325 seems to be more specific, as no functional nAChRs were obtained when they were substituted by alanines (construct 28). This sequence, MKR, or slightly different variants of it, is highly conserved among the different neuronal and nonneuronal nAChR subunits.

nAChRs without the Cytoplasmic Loop Have different Electrophysiological Properties. We next tested whether the absence of a large protein region at the cytoplasmic portion of the nAChR would modify its functional properties. For this purpose, we compared wild-type α7 nAChRs with construct 14, which lacks amino acids 326−370 and 374−432 and produced high levels of nAChR expression. Figure 5A shows the current−voltage relationships for both nAChR-types. In this figure, the average peak current value in response to 1 mM acetylcholine (ACh) is shown for both nAChRs as a function of membrane potential. At this agonist concentration, construct 14 currents were about 5-fold greater than α7, although, as shown below in the dose−response curves, this concentration is not totally equivalent for both nAChRs. The reversal potential was close to zero in both nAChRs; however, rectification in construct 14 was smaller than in α7. The later point can be illustrated, for instance, as the ratio of the values of the chord conductance for inward currents (between −80 and −100 mV) and outward currents (between 20 and 40 mV), that is approximately 4.2 for α7 nAChRs, and only 1.6 for construct 14. Figure 5B shows dose−response curves for peak currents obtained in both nAChRs with ACh at −80 mV. Construct 14 had a smaller EC_{50} (80 μM approximately) and a larger Hill coefficient (about 1.7) than α7 nAChRs (500 μM and 1.1, respectively); thus, 1 mM ACh is a nearly saturating concentration for construct 14, but not for α7 nAChRs. The current records shown in the insets indicate that current kinetics is similar in both nAChRs with faster activation and desensitization at higher concentrations of ACh, although we have not quantified any kinetic parameter. Therefore, we conclude that nAChRs without major fragments of the cytoplasmic loop have some functional properties altered, stressing the relevance of this region not only on the overall structure of the nAChR but also on some of its functional properties.

Specificity of the a7 Subunit Loop versus other Proteins. Since only certain regions of the cytoplasmic loop directly adjacent to transmembrane fragments 3 and 4 appear essential

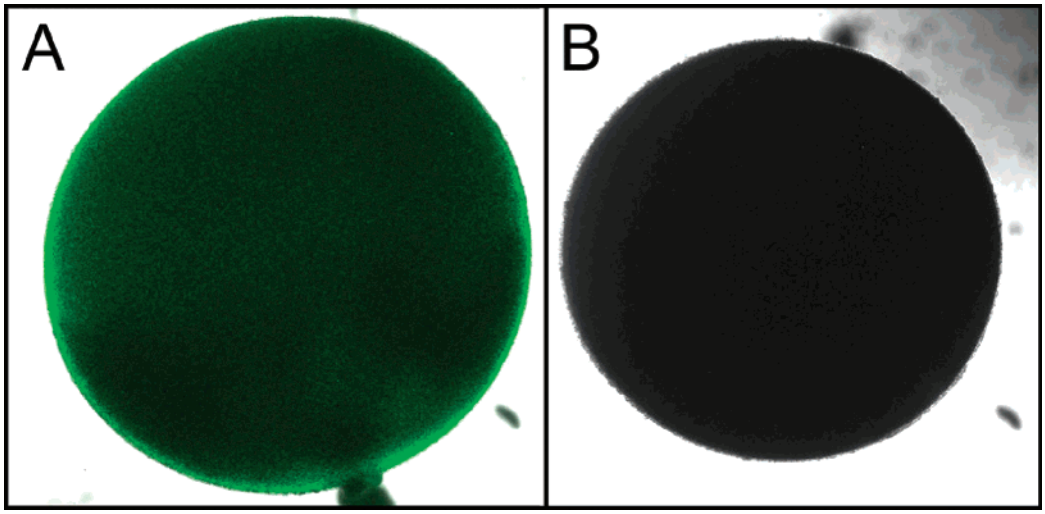

FIGURE 7: Expression of α7-GFP chimeric nAChRs in *Xenopus* oocytes. RNAs coding for construct 30 (panel A) and wild-type α7 subunit (panel B) were injected into *Xenopus* oocytes, and fluorescence was followed by laser confocal microscopy. Oocytes injected with construct 30, which has GFP inserted into the cytoplasmic region of the α7 subunit, showed fluorescence at their external surface, while the ones injected with α7 did not. This pattern was consistently observed in several oocytes from two different donors.

for expression of functional channels, we asked next whether such a "minimal" but sufficient loop would accommodate segments from other proteins, related or not to the nAChR, with the aim of discerning how constrained the nAChR structure is in this region. For this purpose, we designed an intermediate construct that contained several restrictions sites which would be useful for further insertions. The resulting mutant could be also tested, as it represents a substitution of the minimal segment (EGM) needed for high nAChR expression, by another one of seven amino acids (construct 29, Figure 6). On the basis of this construct, we assembled chimeric subunits by inserting proteins such as the whole GFP, the cytoplasmic loops of the α4 and α5 nAChR subunits, and the complete SNAP-25 protein, a SNARE protein involved in exocytosis and anchored at the cytoplasmic face of the membrane through a palmitoyl residue (*22*, *23*). Construct 29 was able to express functional nAChRs at a level close to construct 14; therefore, the substitution mentioned above was not deleterious for nAChR expression. Insertion of GFP (239 amino acids) induced a decrease of about 70% of α-Bgt binding sites at the oocyte membrane, but surface nAChRs were functional (construct 30, Figure 6). Moreover, the expressed construct was fluorescent (Figure 7), suggesting that GFP could be accommodated into the loop and fold properly to yield its typical fluorescence. By contrast, the presence of the α4 subunit loop (226 amino acids, construct 31, Figure 6) strongly reduced α-Bgt binding sites, and no functional nAChRs were detected. The insertion of a much shorter cytoplasmic region, the one corresponding to the α5 subunit (45 amino acids, construct 32, Figure 6) was also deleterious for nAChR expression, and only a small amount of surface nAChRs, some of them functional, was observed. Finally, the construct containing the SNAP-25 protein (construct 33) produced 77% of the α-Bgt binding sites observed with wild-type α7 subunits; however, no functional nAChRs were present at the oocyte membrane. These results indicate that, although relatively large segments of the α7 loop can be deleted without detrimental effects on expression of functional nAChRs, the structure of this region seems to be very restrictive with respect to the insertion of other protein segments of varied origin and length.

DISCUSSION

On the basis of the present study, we propose that a large portion of the cytoplasmic loop of the α7 subunit (amino acids 326−432) is not needed for the expression of functional nAChRs. However, some minimal structural elements within amino acids 297−325 (deleted partially in construct 1) and 437−447 (deleted in construct 2) are required for proper channel expression. These elements are located in the interface between transmembrane fragments M3 and M4 and the cytoplasmic region of the α7 subunit, and their sequences are very conserved among the different nAChR subunits. In a previous study, numerous deletions of the cytoplasmic loop of the *Torpedo* α subunit were analyzed (*24*). Interestingly, a deletion close to the M4 fragment (Δ394−401), which overlaps with the deletion in construct 2, induced a strong decrease in expression, and no functional channels were detected. These protein segments might be involved in processes related to the assembly and/or traffic of nAChRs. For instance, the amino acid K314 of the muscle nAChR α subunit, which is in the cytoplasmic loop, close to transmembrane fragment M3, appears to be involved in endoplasmic reticulum to cell surface trafficking (*8*). This amino acid is not present at the α7 subunit, but others in this area could play an analogous role. Alternatively, these elements might be essential constituents of the overall structure of the nAChR, perhaps forming part of the cytoplasmic mouth of the pore. Within these segments, charged amino acids, that may establish electrostatic interactions among them and also with ions, are frequent; however, their mere presence in the cytoplasmic loop may not be sufficient for proper channel structure. Consider, for instance, the case of the N-terminal region of the loop, where amino acids 326−338 (including five charged ones) could be deleted without consequences (see Figure 2, construct 11), while deletion of amino acids 311−325 (including three charged ones) induced loss of expression (Figure 2, construct 10). Additional experiments in this region (Figure 4) suggested that other factors are more relevant, mainly the need to keep this part of the loop with a minimal length and also the presence of specific amino acids. Thus, in the context of construct 14, which has a

cytoplasmic loop of just 50 amino acids, deletion of only three of them in the segment between amino acids 317 and 322 (Figure 4, constructs 22, 23, and 24) abolished nAChR expression. Since functional expression was restored upon insertion of three alanines or the homologous sequence found in the α3 subunit (constructs 25, 26, and 27), it can be deduced that this region does not require specific amino acids, but rather it had to span a minimal length. By contrast, the adjacent amino acids 323−325 (MKR) cannot be substituted by others. Thus, not only deletion of these residues was detrimental for nAChR expression (construct 27) but also their substitution by three alanines (construct 28). This requirement for α*7* nAChR expression contrasts with results from the deletion study for the *Torpedo* α subunit previously mentioned (*24*), in which the sequence MKR was eliminated (Δ327−334) with only a decrease of about 25% in nAChR expression. However, the fact that our deletions affect five subunits per receptor molecule instead of only two, as in the *Torpedo* receptor, may preclude a direct comparison.

Another finding of this study is the striking increase in functional channel expression observed with some mutants. Deletion of amino acids 399−432 (domain 4, construct 6, Figure 1) provoked a 2-fold increase in expression, whereas the subsequent deletion of amino acids 339−370 (domains 2 and 4, construct 7, Figure 1) increased to about 4-fold the amount of nAChRs found at the oocyte membrane. This increase was also observed in the total amount of expressed nAChRs; therefore, it does not seem to arise from a redistribution between surface and intracellular nAChR pools through any potential improvements in endoplasmic reticulum to cell surface trafficking mechanisms. Deleted nAChRs differ from the wild-type one in some electrophysiological properties (see below); however, these differences would not justify either the large increase in expression levels. A possibility would be that deletions of certain nucleotide sequences coding for the cytoplasmic loop affect the metabolism of the injected mRNA, mainly its stability and/or translational control (see refs *25* and *26* for reviews), resulting in larger amounts of nAChRs synthesized from a given message. Alternatively, the deleted regions could code for certain protein degradation signals which may be operative in unassembled and/or unfolded subunits. For instance, it has been shown that unassembled muscle α subunits are rapidly degraded (*27*, *28*). Consequently, and regarding α7 subunits with the whole cytoplasmic loop, an equilibrium could be considered between those of them producing assembled nAChRs, perhaps through interactions with chaperones (*29*, *30*) and neighboring subunits (*30*), and the ones following rapid degradation pathways (*31*). By contrast, deleted subunits would lack those rapid degradation signals staying available for nAChR assembly for longer time, and, therefore, the amount of functional nAChRs would increase. Further experiments will be required to explore these possibilities.

The above hypothesis suggests that the role of these α7 subunit cytoplasmic regions in critical nAChR processes may be more complex than expected, and, in fact, the deletion and substitution experiments of region 3 (in subunits with regions 2 and 4 also deleted) seem to confirm this assumption since: (a) large segments of this region can be deleted but, at least, the sequence formed by amino acids E371, G372, and M373 need to be present to keep high expression levels (construct 14, Figure 2), (b) E371 and G372 cannot be simultaneously mutated to alanines without abolishing nAChR expression (construct 17, Figure 3), and (c) despite the apparent limitations imposed by the EGM sequence, this can be substituted by another, PMGLEDL (construct 29, Figure 6). This apparent contradiction may be explained by considering that a certain structure, either contributed by the sequence EGM or by other, but certainly not by alanines, is needed during folding, assembly, and/or transport, so that proper nAChR expression occurs. These potential structural restrictions of the α7 cytoplasmic loop were confirmed when we tried to insert several polypeptide chains in a subunit lacking amino acids 326−432. These chimeric proteins could be considered substitutions of the EGM sequence, mentioned above, by relatively long proteins segments of varied origin (Figure 6). None of these insertions produced functional nAChRs at the level of the wild-type α7 subunit and only the one containing the GFP protein (construct 30) yielded a significant amount of current and α-Bgt binding sites at the oocyte membrane. Moreover, the rigid 11-stranded beta barrel and the coaxial helix of GFP (*32*) could be built to produce fluorescent nAChRs (Figure 7). Paradoxically, the insertion of two nAChR subunit loops was deleterious for nAChR expression. The one corresponding to the α4 subunit was chosen because it was similar in length (226 amino acids) to the GFP insertion (239 amino acids); however, only a small amount of α-Bgt binding sites was detected at the oocyte membrane. Likewise, the small loop of the α5 subunit (45 amino acids) was not tolerated. This is in agreement with previous experiments in which the substitution of the whole α7 loop by the α5 loop produced about a 100-fold decrease in currents detected at the oocyte membrane (*6*) and suggests that each subunit or, at least, each subunit group within the nAChR supergene family, may have different and tight structural constraints in the large cytoplasmic loop region.

Deletions in the cytoplasmic loop not only affected nAChR expression levels but also some nAChR functional properties. The current−voltage relation for wild-type α7 nAChRs showed a small inward rectification with a clear nonzero outward conductance. This rectification was further reduced in construct 14, mainly because a relative increase in the outward conductance (Figure 5). A small inward rectification (with a ratio of inward to outward conductances of only 2.5) has also been observed in α-Bgt-sensitive ACh-activated currents in rat tuberomammillary neurons (*33*). This is in contrast with the strong inward rectification present in chick (*34*) or human (*35*) α7 nAChRs expressed in Xenopus oocytes, and also in rat α7 nAChRs expressed in a neuroblastoma cell line (*36*). The mechanism of rectification in α7 nAChRs has been attributed in part to open channel block by internal free Mg^{2+}, and negatively charged glutamate residues located at the inner mouth of the channel are thought to be essential for rectification (*37*). Fifteen out of a total of 19 negatively charged amino acids present in the cytoplasmic loop of the rat α7 subunit were deleted in construct 14; therefore, the reduction of rectification is not surprising. Moreover, recent structural studies of the *Torpedo* nAChR at high-resolution had suggested that narrow openings between α-helical segments forming part of the cytoplasmic wall of the channel might serve as filters to exclude anions and other impermeable species from the vicinity of the pore (*38*). Presumably, the removal of a large portion of the

cytoplasmic loop in construct 14 would leave an nAChR without part of these cytoplasmic structures, and it could be speculated that intracellular ions would access the pore more easily, increasing the outward conductance and, thus, reducing rectification. Finally, the ACh dose−response curves showed a typical low apparent affinity for wild-type α7 nAChRs (*39*), and approximately a 6-fold increase in the apparent affinity for construct 14. This difference could not be attributed to a change in the desensitization kinetics of the currents of these two nAChRs, as they are very similar. Thus, we could hypothesize that in construct 14 some structural changes in the nAChR have altered either the binding site of ACh or the efficacy of the coupling between binding and gating. The former possibility appears less plausible given the long distance between the cytoplasmic loop and the binding site.

In summary, we can conclude that the α7 cytoplasmic loop may perform multiple tasks, either during nAChR biogenesis or during nAChR functioning, suggesting that its role is more complex and dynamic than may have been expected.

ACKNOWLEDGMENT

The expert technical assistance of Eva Martínez and Susana Gerber is acknowledged. We thank Drs. Jim Patrick and Jon Lindstrom for the rat nAChR subunits cDNAs and the mAb 319, respectively, and Dr. J. A. Ortiz for his critical review of the manuscript. The help of Dr. A. Nadal with the confocal microscopy is also appreciated.

REFERENCES

1. Karlin, A. (2002) *Nat. Rev. Neurosci. 3*, 102−114.
2. Corringer, P.-J., Le Novère, N., and Changeux, J.-P. (2000) *Annu. Rev. Pharmacol. Toxicol. 40*, 431−458.
3. Utkin, Y. N., Tsetlin, V. I., and Hucho, F. (2000) *Membr. Cell Biol. 13*, 143−164.
4. Keller, S. H., and Taylor, P. (1999) *J. Gen. Physiol. 113*, 171−176.
5. Yu, X.-M., and Hall, Z. W. (1994) *Neuron 13*, 247−255.
6. Williams, B. M., Temburni, M. K., Levey, M. S., Bertrand, S., Bertrand, D., and Jacob, M. (1998) *Nat. Neurosci. 1*, 557−562.
7. Temburni, M. K., Blitzblau, R. C., and Jacob, M. H. (2000) *J. Physiol. 525.1*, 21−29.
8. Keller, S. H., Lindstrom, J., Ellisman, M., and Taylor, P. (2001) *J. Biol. Chem. 276*, 18384−18391.
9. Colledge, M., and Froehner, S. C. (1997) *J. Neurosci. 17*, 5038−5045.
10. Wecker, L., Guo, X., Rycerz, A. M., and Edwards, S. C. (2001) *J. Neurochem. 76*, 711−720.
11. Domínguez del Toro, E., Juíz, J. M., Peng, X., Lindstron, J., and Criado, M. (1994) *J. Comp. Neurol. 349*, 325−342.
12. Broide, R. S., and Leslie, F. M. (1999) *Mol. Neurobiol. 20*, 1−16.
13. Gerzanich, V., Anand, R., and Lindstrom, J. (1994) *Mol. Pharmacol. 45*, 212−220.
14. Vernallis, A. B., Conroy, W. G., and Berg, D. K. (1993) *Neuron 10*, 451−464.
15. Dineley, K. T., and Patrick, J. W. (2000) *J. Biol. Chem. 275*, 13974−13985.
16. Vicente-Agulló, F., Rovira, J. C., Campos-Caro, A., Rodríguez-Ferrer, C., Ballesta, J. J., Sala, S., Sala, F., and Criado, M. (1996) *FEBS Lett. 399*, 83−86.
17. Krieg, P. A., and Melton, D. A. (1984) *Nucleic Acids Res. 12*, 7057−7070.
18. García-Guzmán, M., Sala, F., Sala, S., Campos-Caro, A., and Criado, M. (1994) *Biochemistry 33*, 15198−15203.
19. Anand, R., Conroy, W. G., Schoepfer, R., Whiting, P., and Lindstrom, J. (1991) *J. Biol. Chem. 266*, 11192−11198.
20. Schoepfer, R., Conroy, W. C., Whiting, P., Gore, M., and Lindstrom, J. (1990) *Neuron 5*, 35−48.
21. McLane, K. E., Wu, X., Lindstrom, J., and Conti-Tronconi, B. M. (1992) *J. Neuroimmunol. 38*, 115−128.
22. Veit, M., Sollner, T. H., and Rothman, J. E. (1996) *FEBS Lett. 385*, 119−123.
23. Lane S. R., and Liu, Y. (1997) *J. Neurochem. 69*, 1864−1869.
24. Mishina, M., Tobimatsu, T., Imoto, K., Tanaka, K., Fujita, Y., Fukuda, K., Kurasaki, M., Takahashi, H., Morimoto, Y., Hirose, T., Inayama, S., Takahashi, T., Kuno, M., Numa, S. (1985) *Nature 313*, 364−369.
25. Mendell, J. T., and Dietz, H. C. (2001) *Cell 107*, 411−414
26. Guhaniyogi, G., and Brewer, G. (2001) *Gene 265*, 11−23.
27. Claudio, T., Paulson, H. L., Green, W. N., Ross, A. F., Hartman, D. S., and Hayden, D. (1989) *J. Cell Biol. 108*, 2277−2290.
28. Blount, P., and Merlie, J. P. (1990) *J. Cell Biol. 111*, 2612−2622.
29. Blount, P., and Merlie, J. P. (1991) *J. Cell Biol. 113*, 1125−1132.
30. Keller, S. H., Lindstrom, J., and Taylor, P. (1996) *J. Biol. Chem. 271*, 22871−22877.
31. Keller, S. H., Lindstrom, J., and Taylor, P. (1998) *J. Biol. Chem. 273*, 17064−17072.
32. Ormo, M., Cubitt, A. B., Kallio, K., Gross, L. A., Tsien, R. Y., and Remington, S. J. (1996) *Science 273*, 1392−1395.
33. Uteshev, V. V., Stevens, D. R., and Haas, H. L. (1996) *Pflugers Arch. 432*, 607−613.
34. Couturier, S., Bertrand, D., Matter, J. M., Hernandez, M. C., Bertrand, S., Millar, N., Valera, S., Barkas, T., and Ballivet, M. (1990) *Neuron 5*, 847−856.
35. Peng, X., Katz, M., Gerzanich, V., Anand, R., and Lindstrom, J. (1994) *Mol. Pharmacol. 45*, 546−554.
36. Puchacz, E., Buisson, B., Bertrand, D., and Lukas, R. J. (1994) *FEBS Lett. 354*, 155−159.
37. Forster, I., and Bertrand, D. (1995) *Proc. R. Soc. London B. Biol. Sci. 260*, 139−148.
38. Miyazawa, A., Fujiyoshi, Y., Stowell, M., and Unwin, N. (1999) *J Mol Biol. 288*, 765−786.
39. Amar, M., Thomas, P., Johnson, C., Lunt, G. G., and Wonnacott, S. (1993) *FEBS Lett. 327*, 284−288.

BI025831R